

Elastic wave propagation along a set of parallel fractures

Seiji Nakagawa, Kurt T. Nihei and Larry R. Myer

Earth Sciences Division, E.O. Lawrence Berkeley National Laboratory,
Berkeley

Abstract.

Previous studies on elastic wave propagation in fractured media have demonstrated that a single planar fracture supports fracture interface waves and that two plane parallel fractures support fracture channel waves. Here, the results are presented for plane wave propagation through an infinite number of plane parallel fractures with equal fracture spacing and fracture stiffnesses. Analysis of the dispersion equations for this fractured system demonstrates that these waves exhibit symmetric and antisymmetric particle motions, degenerate to classical Rayleigh-Lamb plate waves when the fractures are completely open, and possess dispersive velocities that are functions of both the fracture stiffness and spacing. Time-frequency analysis performed on a series of laboratory ultrasonic transmission measurements on a fractured rock analog shows good agreement with the theoretical predictions.

1. Introduction

Rock masses are often fractured with sets of near-parallel, near-equally spaced fractures. These compliant, imperfect interfaces can have a large impact on both the mechanical and hydraulic properties of the rock mass. Seismic (elastic) waves can be an effective tool for locating fractures and characterizing their properties because of the sensitivity of wave velocities, amplitudes and spectral characteristics to the fracture compliance. Fractures can also trap and guide waves, and the behavior of such waves may prove useful for probing the geometrical and mechanical properties of the fractures.

For the characterization of fractures using seismic waves, the effect of fracture properties on wave behavior needs to be described quantitatively. This can be achieved by modeling a fracture as a non-welded interface of negligible thickness described by a simple constitutive model referred to in the literature as linear slip or displacement-discontinuity (D-D) boundary conditions [Schoenberg, 1980; Pyrak-Nolte et al., 1990]. The key parameter of the model, the fracture stiffness (or compliance), can be determined experimentally, or from more detailed fracture models consisting of a distribution of small cracks and contacts along a plane [Hudson et al., 1996; Liu et al., 2000]. Using the D-D model, dispersion equations of the fracture-guided waves can be derived for single fractures (fracture interface waves [Pyrak-Nolte and Cook, 1987]) and a pair of parallel fractures (fracture channel waves [Nihei et al., 1999]). These equations provide predictive capability for the fracture parameters from measured wave properties. However, for wave propagating along a large number of parallel fractures, numerical simulations are usually performed ([e.g., Mal, 1988; Yi et al., 1997]).

In this paper, we present analytical dispersion equations for elastic wave propagation along an infinite series of equally spaced parallel fractures. Similar to classical Rayleigh-Lamb waves propagating along single plates, these waves propagating along parallel layers that are mechanically coupled across fractures also possess symmetric and antisymmetric particle motions. The degree of the coupling can be described quantitatively by the fracture stiffness defined in the D-D model.

2. Dispersion Equations

The general dispersion equations for plane wave propagation in a medium containing equally spaced parallel fractures can be obtained by applying dynamic periodic boundary conditions (i.e., Floquet-Bloch theory [Floquet, 1883]) and displacement-discontinuity boundary conditions [Schoenberg, 1980] to the plane waves within a single layer between two neighboring fractures. The first set of boundary conditions accounts for the periodicity of the fractures, and the second set accounts for the mechanical response of individual fractures. For the case of in-plane wave

propagation, each of these two sets of boundary conditions consists of two independent equations. From these equations, we obtain a homogeneous linear system of equations for four unknown amplitude coefficients of plane waves (for P- and S-waves propagating in the "up" and "down" directions across the fractures). The propagation of multiply scattered waves is described by an effective slowness or wavenumber (Bloch wave number) that is included in the Floquet-Bloch boundary condition. The dispersion equation is obtained by requiring the matrix determinant to vanish, which yields a nonlinear equation for the frequency-dependent effective slowness.

Such an equation can be expressed in terms of dimensionless parameters. For an isotropic, homogeneous and elastic background medium with density ρ and P- and S-wave velocities C_P and C_S , a dimensionless frequency is defined as $\Omega = \omega h / C_S$, where ω is the circular frequency and h is the fracture spacing. For a given fracture-parallel (x -direction) component of dimensionless slowness ξ_x (normalized by the S-wave slowness), the fracture-normal (z -direction) components of the dimensionless P- and S-wave slownesses within intact layers are $\xi_z^P \equiv \sqrt{\zeta^2 - \xi_x^2}$ and $\xi_z^S \equiv \sqrt{1 - \xi_x^2}$, respectively, where $\zeta \equiv C_S / C_P$. By introducing the z -direction dimensionless effective slowness $\hat{\xi}_z$, the phase difference in the particle motions over a single fracture spacing is $e^{i\Omega \hat{\xi}_z}$. For a single fracture, dimensionless fracture stiffnesses or impedance ratios are given by $\beta_{jj}^S \equiv 2\kappa_{jj} / \omega \rho C_S$ ($j=x, z$), where κ_{jj} are normal ($j=z$) and shear ($j=x$) components of the fracture stiffness defined by the displacement-discontinuity boundary conditions

$$\kappa_{jj}(u_j^+ - u_j^-) = \sigma_{zj} \quad (1)$$

$$\sigma_{zj} \equiv \sigma_{zj}^+ = \sigma_{zj}^- \quad (2)$$

Superscripts $^+$ and $^-$ indicate opposing surfaces of the fracture, and u_j and σ_{zj} are the j -components of displacement and stress on each surface, respectively.

Using the parameters defined above, the dispersion equations for wave propagation within this fractured medium is [Schoenberg, 1983; Nakagawa et al., 2002]

$$F \equiv A \cos^2 \Omega \hat{\xi}_z + B \cos \Omega \hat{\xi}_z + C = 0 \quad (3)$$

where A , B , and C are nonlinear functions of β_{ji}^S and ξ_x but not $\hat{\xi}_z$. Because the fracture-normal component of group velocity needs to vanish for the waves propagating parallel to the fractures, the following condition can be imposed:

$$\partial F / \partial \hat{\xi}_z = -\Omega \sin \Omega \hat{\xi}_z \cdot (2A \cos \Omega \hat{\xi}_z + B) = 0. \quad (4)$$

This equation yields the following three groups of conditions:

$$\text{i) } \Omega \hat{\xi}_z = 2m\pi, m=0,1,2,\dots \quad (5)$$

$$\text{ii) } \Omega \hat{\xi}_z = (2m+1)\pi, m=0,1,2,\dots \quad (6)$$

$$\text{iii) } \Omega \hat{\xi}_z = \cos^{-1}(B/2A). \quad (7)$$

In equations (5) and (6), only non-negative slownesses were specified because negative slownesses lead to the same results as the positive slownesses with the same magnitude. The first condition implies that particle motions within any neighboring two layers are identical because their particle motions are related by the effective slowness as $u_j(z+h)=u_j(z) e^{i\Omega \hat{\xi}_z}=u_j(z)$. Because the phase of the motions is identical, we call the wave satisfying these conditions the "0-mode." The second condition implies that the wave particle motions are 180° out of phase (i.e., $u_j(z+h)=u_j(z) e^{i\Omega \hat{\xi}_z}=-u_j(z)$), and we call this wave the " π -mode." The third condition implies more complicated non-linear dependency of $\hat{\xi}_z$ on the unknown variable ξ_x , that is beyond the scope of this paper (a limited discussion is provided in [Nakagawa, 1998]). For the first two conditions, equation (3) can be factored into two terms as

$$F = (\beta_{zz}^S \xi_z^P + f_p)(\beta_{xx}^S \xi_z^S + f_q) = 0. \quad (8)$$

For the "0-mode", by introducing equation (5), the functions f_p and f_q in equation (8) become

$$f_p = (1 - 2\xi_x^2)^2 \cdot \cot(\Omega \xi_z^P / 2) + 4\xi_x^2 \xi_z^P \xi_z^S \cdot \cot(\Omega \xi_z^S / 2), \quad (9)$$

$$f_q = (1 - 2\xi_x^2)^2 \cdot \cot(\Omega \xi_z^S / 2) + 4\xi_x^2 \xi_z^P \xi_z^S \cdot \cot(\Omega \xi_z^P / 2). \quad (10)$$

It should be noted that the solution of equations $f_p=0$ and $f_q=0$ are the symmetric modes (S-modes) and antisymmetric modes (A-modes) of classical Rayleigh-Lamb plate waves. It can be shown that the particle motions of the mode for the dispersion equation $\beta_{zz}^S \xi_z^P + f_p = 0$, which is a function of the normal fracture stiffness κ_{zz} , are also symmetric within individual layers.

Likewise, the dispersion equation $\beta_{xx}^S \xi_z^S + f_q = 0$ depends on the shear fracture stiffness κ_{xx} , and provides particle motions that are antisymmetric.

For the " π -mode", the condition given by equation (6) leads to equations

$$f_p = -\left[(1 - 2\xi_x^2)^2 \cdot \tan(\Omega \xi_z^P / 2) + 4\xi_x^2 \xi_z^P \xi_z^S \cdot \tan(\Omega \xi_z^S / 2)\right], \quad (11)$$

$$f_q = -\left[(1 - 2\xi_x^2)^2 \cdot \tan(\Omega \xi_z^S / 2) + 4\xi_x^2 \xi_z^P \xi_z^S \cdot \tan(\Omega \xi_z^P / 2)\right]. \quad (12)$$

In contrast to the "0-mode," $f_q = 0$ is the symmetric mode (Rayleigh-Lamb wave), and so is the shear stiffness dependent mode $\beta_{xx}^S \xi_z^S + f_q = 0$. Similarly, $f_p = 0$ and $\beta_{zz}^S \xi_x^S + f_p = 0$ (normal-stiffness dependent) are antisymmetric. Figure 1 summarizes general mode shapes for the "0-mode" and " π -mode," with symmetric and antisymmetric particle motions.

These "generalized" Rayleigh-Lamb plate waves can also be viewed as a generalization of the fracture-guided waves for single fractures (fracture interface waves). However, they may not deserve the title of "guided" waves in the classical sense because the waves are assumed to be present throughout the fractured media.

3. Examples

Dispersion equation (8) with functions given by equations (9) to (12) can be solved to obtain multiple values of the fracture-parallel slowness ξ_x for given values of fracture stiffness, spacing and wave frequency. Once a slowness is obtained, the group velocity in the fracture-parallel direction is obtained through the relationship (e.g., [Schoenberg and Muir, 1989])

$$C_{gx} = \frac{\partial \omega}{\partial k_x} = -\frac{\partial f / \partial k_x}{\partial f / \partial \omega} = \frac{\partial f / \partial \xi_x}{\xi_x (\partial f / \partial \xi_x) + \hat{\xi}_z (\partial f / \partial \hat{\xi}_z) - \omega (\partial f / \partial \omega)} \cdot C_s. \quad (13)$$

where k_x is the fracture-parallel wavenumber and $f=0$ is the dispersion equation.

To examine the effect of fracture stiffness on the dispersion of the waves, it is convenient to define dimensionless fracture stiffnesses $b_{jj} \equiv \kappa_{jj} h / C_s$ ($j=x,z$) which are independent of wave frequency. In the examples shown in Figure 2, the effect of fracture stiffness on the group velocity dispersion of the four types of the generalized Rayleigh-Lamb waves is examined for a material with a Poisson's ratio equal to 0.2. Normal and shear fracture stiffnesses are assumed to

be equal ($b \equiv b_{zz} = b_{xx}$). In the figure, the m^{th} mode of each mode type is labeled as, $Sm-0$, $Sm-\pi$, $Am-0$ and $Am-\pi$. From the figure, as the fracture stiffnesses approach zero, the $Sm-0$ and $Sm-\pi$ modes degenerate to single symmetric Rayleigh-Lamb modes, and the $Am-0$ and $Am-\pi$ modes to antisymmetric Rayleigh-Lamb modes, respectively. In contrast, in the high-stiffness limit, a part of the $S0-0$ and $S1-0$ modes becomes a P-wave, and the $A0-0$ mode becomes an S-wave. Other symmetric and antisymmetric modes with the same order and phase difference (i.e., 0- and π -modes) degenerate to single modes.

To demonstrate the existence of the generalized Rayleigh-Lamb wave within a medium containing parallel fractures, we conducted laboratory experiments on an idealized fractured medium consisting of a stack of roughened steel plates. The surfaces of each plate were sand-blasted to produce compliant interfaces. The thickness of individual plates was 3.18 mm, the width and height was 10.16 cm. Measured P- and S-wave velocities of the steel were 5901 m/sec and 3243 m/sec, respectively. This sample was the same one used in the experiment reported by *Pyrak-Nolte et al. (1990b)*. In addition to this sample, a single plate (thickness 3.40 mm, length 10.2 mm) and an intact steel cylinder (diameter 10.2 cm, length 8.65 cm) were also tested for comparison, representing the cases for zero and infinite fracture stiffnesses, respectively.

During the test, a pair of piezoelectric transducers with a central frequency of 1 MHz was clamped on the sides of the sample (Figure 3), and waves transmitted along the model fractures were measured for different axial loads (0 kN and 50 kN) to examine the dispersion of the waves at different fracture stiffnesses.

For the P-wave source with the wavelength close to the plate thickness, the dispersion was the strongest for the single plate, and was not present for the intact block (Figure 4). Also, for all the cases except for the reference “intact” case, the first-arriving part of the waveforms contained higher frequencies than the later part. To have a better understanding of the velocity dispersion of the measured waves, we performed a time-frequency analysis using a moving window maximum entropy method (e.g., [*Burg, 1967*]) (Figure 5). From the plots, systematic changes in

the group velocity dispersion of the waves propagating along the fractures can be seen as the fracture stiffness is increased. The superposed type curves were computed using the equations (9) and (13). From the experimentally measured dispersion of the waves, we identify the first-arriving, high-frequency part of the waves in Figure 4 as mostly the S1-0 mode, and the subsequent strongly dispersive part as the S0-0 mode. Antisymmetric (A-) and “ π -“ modes were not considered here because the geometry of the source does not allow the generation of these modes. By using a series of type curves for the theoretical dispersion and comparing them with the experimentally measured dispersion, the fracture stiffness can be determined. For the example examined above, the dimensionless normal stiffness of the fractures was approximately $b_{zz}=1$ for the normal load of 0 N, and $b_{zz}=2$ for 50 kN.

4. Conclusions

In this paper, we presented closed-form dispersion equations for elastic wave propagation along an infinite series of equally spaced, plane-parallel fractures, and examined the dispersion of the waves as a function of fracture stiffness. Our analysis showed that these waves are Rayleigh-Lamb plate waves (or Lamb waves) generalized for finite fracture stiffness. An important result is that the dispersion of these new waves can be used to determine the fracture stiffness of the fractures with a known fracture spacing. Furthermore, because different modes of these waves depend on either normal or shear fracture stiffness, as with the fracture interface waves propagating along a single fracture ([*Pyrak Nolte and Cook, 1987*]), the normal and shear fracture stiffness can be determined independently from the dispersion of different modes. We demonstrated this by determining the normal fracture stiffness of a fractured rock analog using the dispersion of the lowest-order symmetric mode.

Acknowledgments

This research was supported by the Director, Office of Energy Research, Office of Basic Energy Sciences under U.S. Department of Energy Contract No. DE-AC03-76SF00098.

References

- Burg, J. P., Maximum entropy spectral analysis, presented at the Int. Meeting Soc. Explor. Geophys., Orlando, FL, 1967.
- Floquet, G., Sur les équations différentielles linéaires à coefficients périodiques, *Annal. Ecole Normale*, 12, 47-89, 1883.
- Hudson, J. A., E. Liu and S. Crampin, Transmission properties of a plane fault, *Geophys. J. Int.*, 125, 559-566, 1996.
- Liu, E., J. A., Hudson and T. Pointer, Equivalent medium representation of fractured rock, *J. Geophys. Res.*, 105, 2981-3000, 2000.
- Mal, A. K., Guided waves in layered solids with interface zones, *Int. J. Engng. Sci.*, 26(8), 873-881, 1988.
- Nakagawa, S., *Acoustic Resonance Characteristics of Rock and Concrete Containing Fractures*, Ph.D. Thesis, Univ. of California at Berkeley, 1998.
- Nakagawa, S., K.T. Nihei, and L.R. Myer, Frequency-dependent anisotropic wave propagation in media containing equally spaced multiple parallel fractures, submitted to *Geophys. J. Int.*, 2002.
- Nihei, K. T., W. Yi, L. R., Myer, N. G. W., Cook and M. Schoenberg, Fracture channel waves, *J. Geophys. Res.*, 104, 4769-4781, 1999.
- Pyrak-Nolte, L. J., L. R. Myer, and N. G. W. Cook, Transmission of seismic waves across single fractures, *J. Geophys. Res.*, 95, 8617-8638, 1990a.
- Pyrak-Nolte, L. J., L. R. Myer, and N. G. W. Cook, Anisotropy in seismic velocities and amplitudes from multiple parallel fractures, *J. Geophys. Res.*, 95, 11345-11358, 1990b.
- Pyrak-Nolte, L. J. and N. G. W. Cook, Elastic interface waves along a fracture, *Geophys. Res. Lett.*, 14, 1107-1110, 1987.
- Schoenberg, M., Elastic wave behavior across linear slip interfaces, *J. Acoust. Soc. Am.*, 68(5), 1516-1521, 1980.

Schoenberg, M., Reflection of elastic waves from periodically stratified media with interfacial slip, *Geophys. Prospect.*, 31, 265-292, 1983.

Schoenberg, M. and F. Muir, A calculus for finely layered anisotropic media, *Geophys.*, 54(5), 581-889, 1989.

Yi, W., S. Nakagawa, K. T. Nihei, J. W. Rector, L. R. Myer, and N. G. W. Cook, Numerical investigation of fracture-induced seismic anisotropy, 67th SEG Extended Abstracts, 960-963, 1997.

S. Nakagawa, K. Nihei, and L. Myer, Earth Sciences Division, E. O. Lawrence Berkeley National Laboratory, Berkeley, CA 94720 (e-mail: snakagawa, ktneihei, or lmyer@lbl.gov)

(Received ; revised; accepted)

NAKAGAWA ET AL.: WAVE PROPAGATION ALONG PARALLEL FRACTURES

Figure 1. Schematic plots of mode shapes for the four types of fracture stiffness-dependent, generalized Rayleigh-Lamb modes.

Figure 2. Theoretical dispersion curves for the group velocities of generalized Rayleigh-Lamb waves, as a function of dimensionless fracture stiffness b . Poisson's ratio of the material is assumed to be 0.2.

Figure 3. Experimental setup for measuring the dispersive group velocities of guided waves propagating in a medium with equally-spaced, plane-parallel fractures.

Figure 4. Measured waveforms for compressional transducers at different loads. Note that the propagation distance is slightly different for different samples (see text).

Figure 5. Group velocity dispersion curves obtained from time-frequency analysis of the measured waveforms. Dark colors indicate high wave energy, and each plot is normalized to the highest value of the plot.

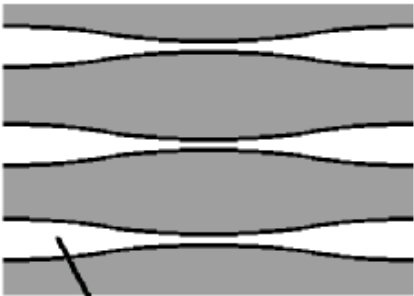
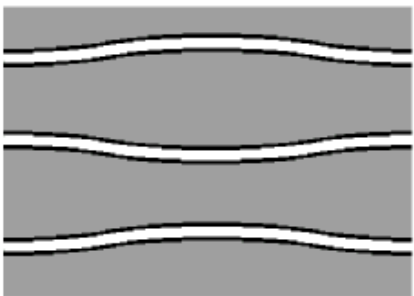
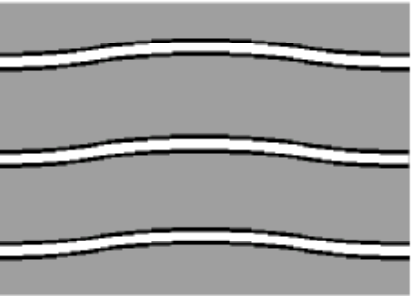
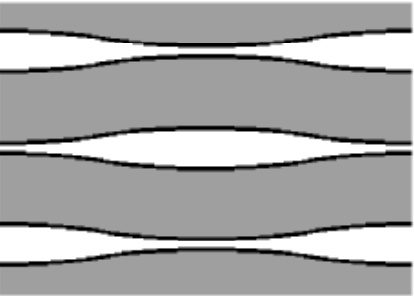
	in-phase (0-mode)	out-of-phase (π -mode)
symmetric (S-mode)	 <p>fracture</p>	
anti-symmetric (A-mode)	 <p>z x</p>	

Figure 1.

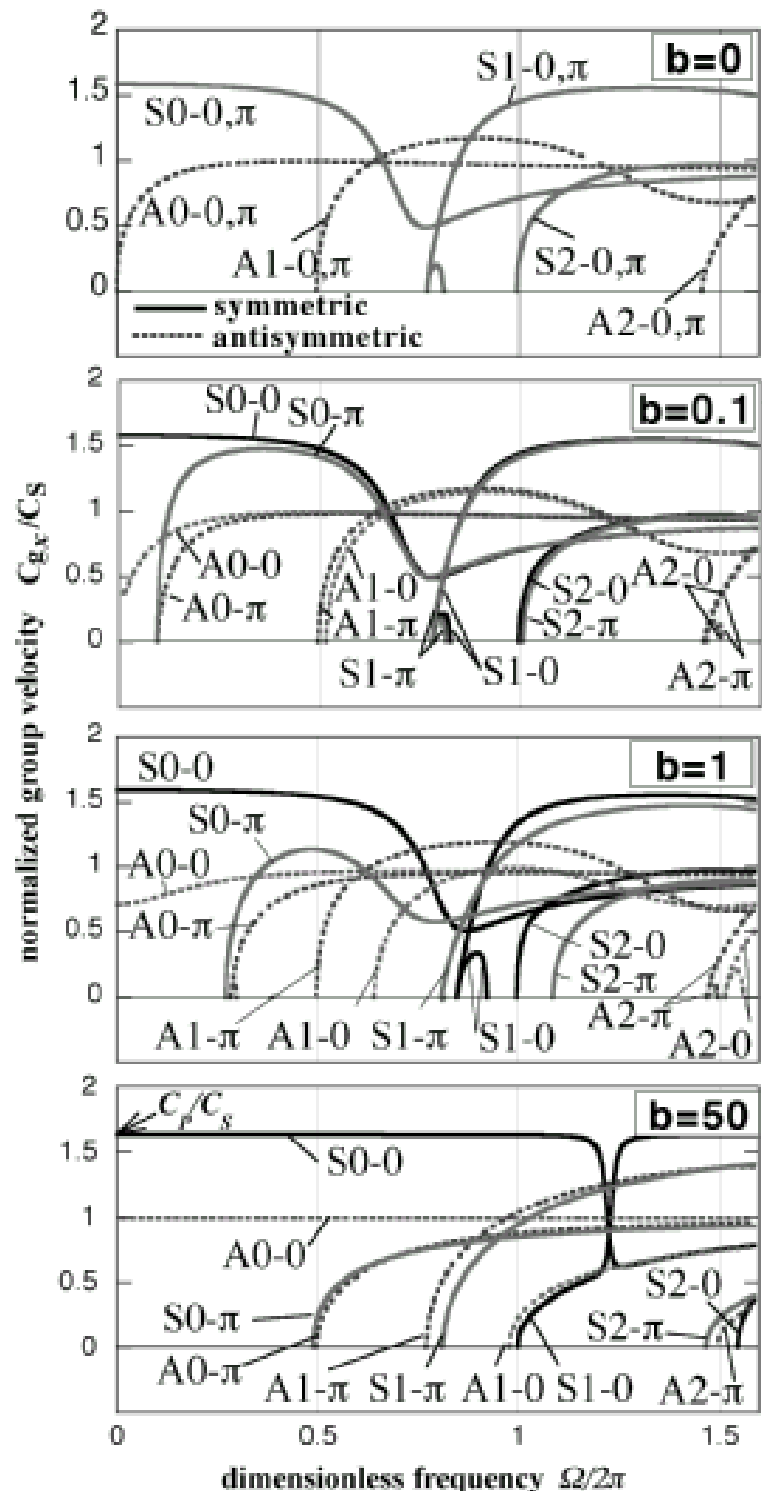


Figure 2

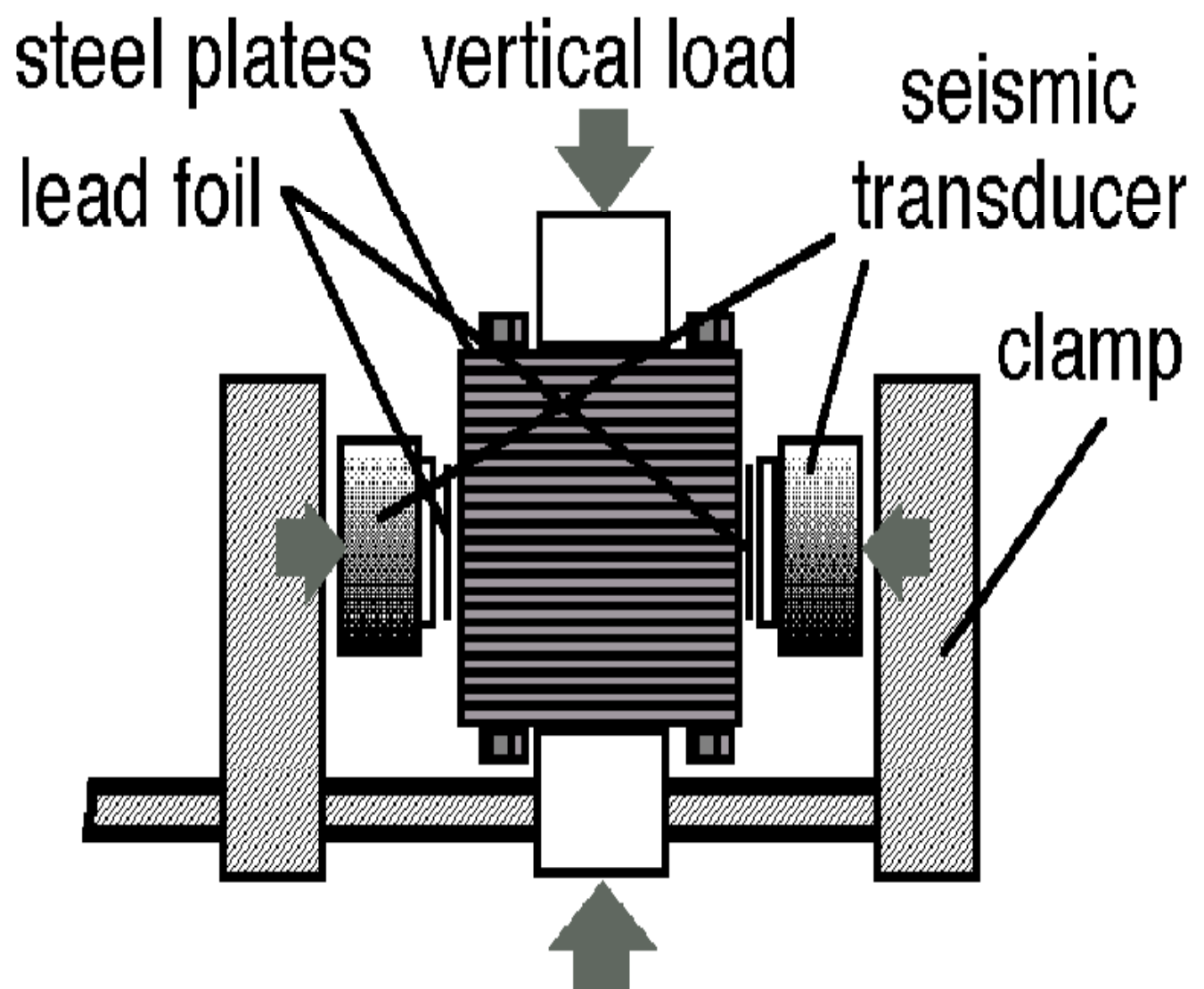


Figure 3

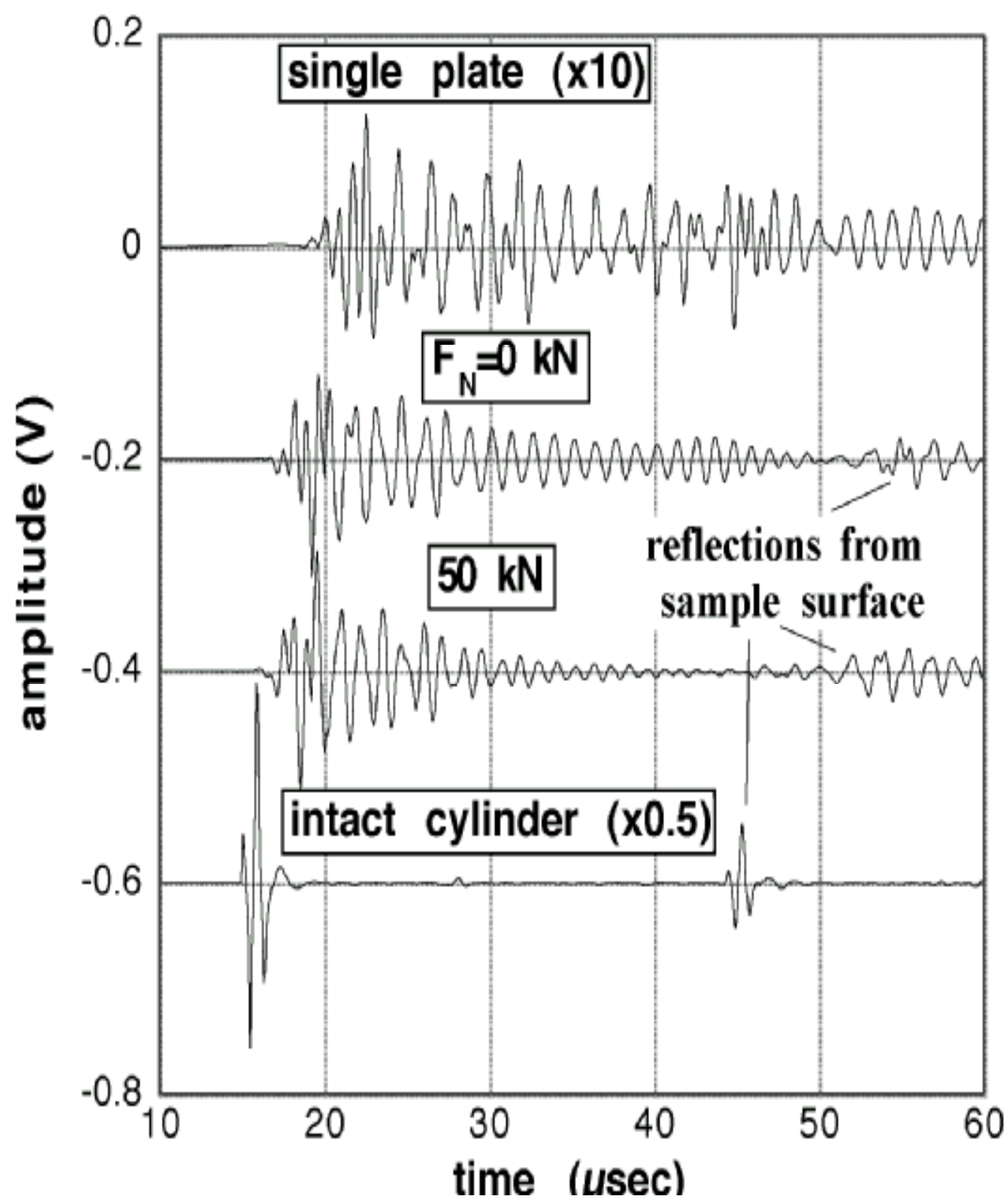


Figure 4.

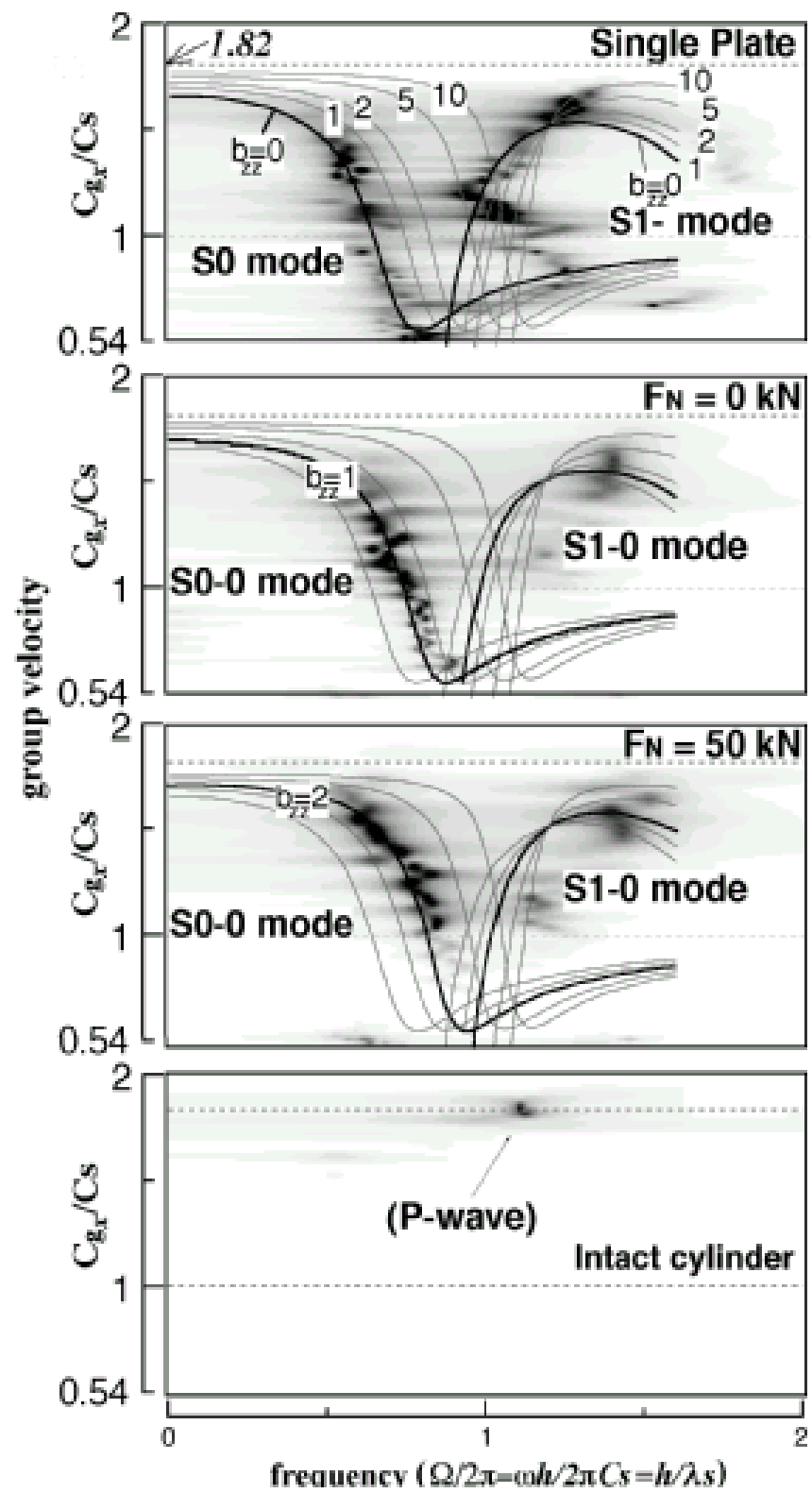


Figure 5.